Society For Biomaterials

VEGF release from a polymeric nanofiber scaffold for improved angiogenesis

Hadar Zigdon-Giladi,[1,2,3] Alaa Khutaba,[1,2,3] Rina Elimelech,[1,2] Eli E. Machtei,[1,2,3] Samer Srouji[4,5]

[1]Department of Periodontology, School of Graduate Dentistry, Rambam Health Care Campus, Haifa, Israel
[2]Research Institute for Bone Repair, Rambam Health Care Campus, Haifa, Israel
[3]The Rappaport Family Faculty of Medicine, Technion, Israel Institute of Technology, Haifa, Israel
[4]Chief of Oral and Maxillofacial Department, Bone Research Laboratory, Galilee Medical Center, Nahariya, Israel
[5]Faculty of Medicine in the Galilee, Bar-ilan University

Received 1 March 2017; revised 3 May 2017; accepted 23 May 2017
Published online 21 June 2017 in Wiley Online Library (wileyonlinelibrary.com). DOI: 10.1002/jbm.a.36127

Abstract: Angiogenesis plays a pivotal role in tissue engineering and regenerative medicine. This study aimed to develop an electrospun fiber scaffold that supports release of recombinant human vascular endothelial growth factor (rhVEGF) to enhance angiogenesis. Scaffolds composed of core–shell fibers were fabricated using co-electrospinning. The core solution was composed of polyethylene oxide and mixed with rhVEGF. The shell solution was composed of polycarpolactone, with 0.25, 1, and 3% of polyethylene glycol (PEG) to manipulate pore size on the shell. Pore size and density increased with higher PEG concentrations. Similarly, rhVEGF release was affected by PEG concentration: initial burst release was found in all scaffolds, followed by continuous 4 h release in 3% PEG and 18 h release in the 0.25 and 1% PEG polymeric scaffolds. Endothelial cell migration toward rhVEGF-incorporated polymeric scaffold was 80-fold higher as compared to VEGF-free polymeric scaffold. In a subcutaneous mouse model, VEGF-incorporated polymeric scaffold stimulated cell migration into the scaffold within three days and significantly enhanced blood vessels formation within 14 days, whereas control scaffolds contained few vessels. In conclusion, the described novel scaffold represents a promising device for vascular tissue engineering, which may be of clinical significance in treating vascular deficient wounds. © 2017 Wiley Periodicals, Inc. J Biomed Mater Res Part A: 105A: 2712–2721, 2017.

Key Words: angiogenesis, recombinant human vascular endothelial growth factor, nanofibers scaffold, co-electrospinning, tissue engineering

How to cite this article: Zigdon-Giladi H, Khutaba A, Elimelech R, Machtei EE, Srouji S. 2017. VEGF release from a polymeric nanofiber scaffold for improved angiogenesis. J Biomed Mater Res Part A 2017:105A:2712–2721.

INTRODUCTION

The continuously evolving multidisciplinary field of tissue engineering aims to develop biological substitutes to restore, replace or regenerate defective tissues.[1] In all fields of regenerative medicine and wound healing, efficient blood supply is essential for delivery of nutrients, oxygen and cells to regenerating sites. Yet, most engineered grafts are nonvascularized, forcing the transplanted site to rely solely on diffusion of oxygen from the recipient bed, restricting the source to a maximum distance of 100–200 μm^2.[2] The development of a vascular system is critical to ensure oxygen supply to maintain the survival and function of the cells,[3–5] and usually requires 4 days.[6] Numerous techniques to enhance graft vascularity have been investigated. The use of vascularized grafts has shown promising results, however, it is not always feasible. The process is technique-sensitive, limited by donor site availability and associated with high patient morbidity.[7] Alternative techniques include engineered vascularized grafts, integrating cells, scaffolds and growth factors.[7,8]

Primary cells involved in angiogenesis and vasculogenesis include endothelial cells (EC) or smooth muscle cells (SMC). Vascular endothelial growth factor (VEGF) is the growth factor most dominantly involved in the process of angiogenesis, as it is a potent inducer of EC proliferation, migration and tube formation.[9–11] Other growth factors which are imperative to angiogenesis include insulin growth factor (IGF), fibroblast growth factor (FGF), platelet-derived growth factor (PDGF), stromal cell-derived growth factor (SDF), and hepatocyte growth factor (HGF). VEGF is produced by many cell types including tumor cells, macrophages, platelets, keratinocytes, and renal mesangial cells. The activities of VEGF are not limited to the vascular system; VEGF plays a role in normal physiological functions such as bone formation, hematopoiesis and wound healing. The VEGF family currently includes six known members: VEGF-A through E and placental growth factor. VEGF-A is most prevalent and consists of five isoforms of which $VEGF_{165}$ is the predominant molecular species.[9,10,12] Cell hypoxia triggers the release of hypoxia-inducible factor (HIF), a transcription factor which stimulates the release of VEGF-A. Circulating VEGF-A binds to VEGF receptors on endothelial cells, triggering a tyrosine kinase-dependent pathway, which initiates angiogenesis. The major impediment to the use of VEGF in tissue engineering is its relatively short half-life ($hVEGF_{165}$: 33.7 $\pm$ 13.7 min).[13]

Correspondence to: H. Zigdon Giladi; e-mail: hadar@tx.technion.ac.il

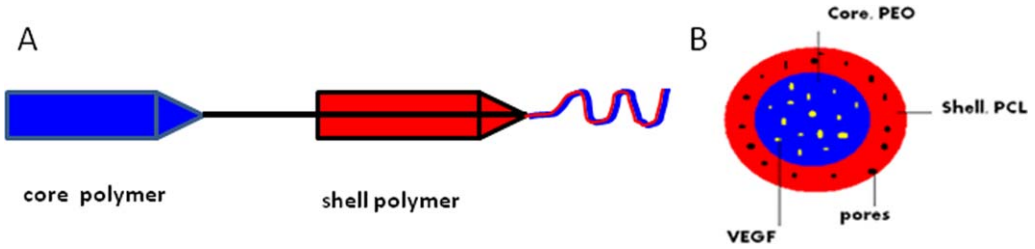

FIGURE 1. Schematic presentation of the co-electrospinning process. A: Two syringes, one containing the shell polymer solution, and the other containing the core solution, simultaneously inject the solutions into the electrostatic field. B: Cross-section of the fibers, showing the solidified shell surrounding a softer core that contains VEGF. Small pores are present in the outer shell.

Controlled-release scaffolds have been proposed as a feasible means of overcoming this obstacle. Electrospinning is a cost-efficient technique for producing interconnected and highly porous, nanometer, polymeric fibrous scaffolds,[9] that mimic the architecture of the extracellular matrix (ECM). An advanced electrospinning technique involves the co-spinning of two polymers which creates a core–shell fiber scaffold. Core–shell fiber scaffolds consist of a stiff polymer outer shell surrounding a softer polymer core. The core polymer is doped with the molecule to be delivered, while the shell is designed to be porous, to allow the core to degrade and release the molecule.[14–16] The main advantage of these electrospun core–shell systems lies in the ability to control the release of soluble molecules by tailoring the different polymer concentrations to fit the release profile of the molecules within the time-frame of tissue regeneration.[17]

Previous studies have shown that burst release of high concentrations of VEGF may induce formation of hemangiomas and malformed vessels.[18] In contrast, sustained release of low doses of VEGF is preferable. This study aimed to design a nanofiber polymeric scaffold that allows for slow and steady release of VEGF, in order to promote the production of vascular networks within the implanted scaffold.

MATERIALS AND METHODS

The study protocol was approved by the Committee for the Supervision of Animal Experiments at the Faculty of Medicine, Technion, I.I.T. (approval # IL0530412).

Electrospinning for scaffold fabrication

Core–shell fiber scaffolds were fabricated using a co-electrospinning technique, as previously described by Dror et al.[19] Scaffold fabrication was performed at room temperature (23°C) and relative humidity of 40–45%. The spinning parameters were: electrostatic field of 0.65 kV/cm, and the distance between the spinneret and the collector was 10 cm. The flow rate for both the core and the shell was controlled by two syringe pumps; the flow rate for the shell was 3.0 mL/h and for the core 0.3 mL/h. The fibers were collected as long strips on the surface of a vertical rotating disc with a diameter of 4 cm and width of 1.1 cm that enabled the formation of a scaffold containing preselected amount of growth factors/cm^2.

The shell solution was composed of 8 wt % polycaprolactone (Sigma-Aldrich, Munich, Germany) 80 K and 0.25–3 wt % polyethylene glycol (PEG) (Sigma-Aldrich, Munich, Germany) 6 K, dissolved in a 8:2 (w/w) mixture of chloroform and dimethyl formamide (Sigma-Aldrich, Munich, Germany). Various weight concentrations of PEG (0.25%, 1%, 3%) were used in order to fabricate scaffolds with different pore sizes on the surface of the shell. The core solution was composed of 4 wt % (polyethylene oxide) (PEO) 600 K, dissolved in deionized water. This co-electrospinning process allows for the fabrication of nanofiber scaffolds that consist of an external perforated shell and internal core. rhVEGF$_{165}$ [R&D systems (Minneapolis, MN, USA; 1.35 or 0.25 μg/mL) was added to the core solution (Fig. 1). The addition of 0.25 μg/mL hrVEGF to the core solution results in 2.5 ng VEGF/cm^2 scaffold. This concentration was used for ELISA analysis in order to monitor the release kinetics of VEGF from the scaffold. This concentration allowed VEGF concentrations to be within the ELISA assay range. In the trans-well migration assay and the *in vivo* model, higher concentration of VEGF was used in order to achieve a biological effect (15 ng hrVEGF/cm^2 scaffold was achieved by adding 1.35 μg/mL hrVEGF to the core solution).

Scanning electron microscopy imaging

Scaffolds were immersed in water to dissolve the PEG polymer and to open the pores. Images of the fibers were obtained using a Leo Gemini high-resolution scanning electron microscope (SEM), set at an acceleration voltage of 3 kV with magnifications of: 10, 50, 100 K

Determining rhVEGF$_{165}$ release from the scaffold

One cm^2 scaffold that was loaded with 2.5 ng rhVEGF$_{165}$/cm^2 was placed in PBS as a releasing buffer (pH 7.4). Samples were collected at various time intervals (immediately, 2, 8, 14, 26 h) and frozen: an enzyme-linked immunosorbent assay (ELISA) (R&D System, Minneapolis, USA) was conducted according to the manufacturer's instructions.rhVEGF$_{165}$ concentration was determined at OD$_{450nm}$, using a standard spectrophotometer. The concentrations of rhVEGF$_{165}$ in samples were calculated from a 7-point standard curve obtained from serially diluted hVEGF$_{165}$ (initial concentration of 1000 pg/mL).

Cell adherence to the scaffold

Human bone marrow derived Stromal cells were isolated and characterized as previously described.[20] 1×10^4 stromal cells were labeled with the cytoplasmic dye carboxyfluorescein

succinimidyl ester (CFSE) (Invitrogen) and seeded on 0.5 cm^2 VEGF-free scaffolds. Before seeding, the scaffold was stained with Dil (Molecular Probes, Eugene, OR, USA) as follows: 0.5 cm^2 scaffold was soaked in 1 μL Dil/mL PBS for 1 min and then washed with 10 mL PBS. Stained MSC-seeded scaffolds were incubated for 24 h. Nonadhered cells were removed by gentle washing with PBS. Before visualization under the microscope, the scaffolds were soaked in Hoechst stain (Sigma-Aldrich, St. Louis, USA). To demonstrate cell adhesion to the scaffold, an LSM 700 Zeiss laser scanning confocal system was used. The lasers used were 405, 488, 555, and the emission wavelengths $\geq$420, $\leq$540, $\geq$560 nm, respectively. Images were processed using the Imaris software (Bitplane, Zurich, Switzerland).

In vitro rhVEGF$_{165}$ bioactivity trans-well migration assay

The Millipore 12-well millicell trans-well migration assay kit (Millipore Corporation, Billerica, MA), with an 8 μm pore size, was used. The membrane was coated with 5 μg/cm^2 fibronectin (Biological Industries, Beit Haemek, Israel). Endothelial cells (5×10^4) (kindly provided by Dr. Mazid Falah) were seeded on top of the porous membrane, in serum-free endothelial cell basal medium-2 (EBM-2) (Lonza, Walkersville, MD, USA). Cells were seeded on top of the porous membrane and then incubated and allowed to adhere overnight. In order to investigate the migratory response of endothelial cells through the membrane, an examined chemotactic agent was placed on the lower side of the membrane: (1) EBM-2 without supplements, (2) EBM-2 with 5 ng/mL rhVEGF$_{165}$ (this concentration was used based on the literature, (3) 1% PEG polymeric scaffold previously incorporated with 15 ng/cm^2 rhVEGF$_{165}$ soaked in EBM-2 without supplements, (4) scaffold without VEGF, soaked in EBM without supplements. Three duplicates for each group were tested in a single assay. The system was then incubated for 24 h. At the end of incubation, cells on the inserts were fixed and stained with crystal violet (Merck KGaA, Darmstadt, Germany).

To quantify the number of cells that passed through the porous membrane, Image Pro-Premier software was used to measure the total violet color area (represents cells), divided by the total image area.

In vivo rhVEGF$_{165}$ bioactivity assays

Severe combined immunodeficiency (SCID) mice ($n = 12$, 12-week-old, 200 g weight) were allocated into two groups: control ($n = 6$)—subcutaneous transplantation of 1% PEG polymeric scaffold (0.5 cm^2) without VEGF and test ($n = 6$)—subcutaneous transplantation of 1% PEG polymeric scaffold (0.5 cm^2) incorporated with 15 ng/cm^2 rhVEGF$_{165}$. Five subcutaneous pouches were performed on the back of each mouse and 0.5 cm^2 scaffold was inserted into each pouch. The skin was sutured with horizontal mattress sutures for minimal tension, using resorbable vicryl 5–0 sutures (Ethicon, US, LLC). Throughout the entire experiment, each mouse was kept in a separate cage. Three mice from each group were sacrificed after 3 and 14 days. Mice were anesthetized with an intramuscular injection of ketamine (Ketaset, Fort Dodge, IO, USA; 10 mg/100 g body weight) and xylazine (Eurovet, Cuijk, Holland; 0.5 mg/100 g body weight). Upon scarification mice were injected with fluorescein isothiocyanate-dextran (Sigma-Aldrich, USA), with a molecular weight of 500,000, to label the functional blood vessels. Moreover, subcutaneous transplants were extracted and prepared for histological evaluation.

Dextran preparation and injection

Dextran was dissolved in PBS to a final concentration of 10 mg/mL, of which 0.2 mL was injected in the tail vein 8 s before sacrifice. Functional blood vessels were visualized with an LSM 510 laser scanning confocal system (Zeiss, Oberkochen, Germany), using laser wavelengths 405, 488, 561, and 633 nm. Band-pass emission filters 420–480, 505–550, 575–615IR, and long-pass emission filters $\geq$650 nm, respectively were used. All samples were observed using a 25/0.8 oil immersion objective lens. Images were processed and analyzed using the Imaris software (Bitplane, Zurich, Switzerland), that enabled measurement of total blood vessel area, total blood vessel length, total blood vessel volume, number of blood vessel branches and total blood vessel diameter.

Histological preparation

The specimens were fixed with 4% paraformaldehyde, embedded in paraffin, sectioned (5 μm) and stained with Hematoxylin and Eosin (H&E). Five H&E-stained regions from each specimen were imaged using a 3D Histech Pannoramic MIDI (3DHISTECH, Budapest, Hungary) scanner that uses a Plan-Apochromat $\times$20/0.8 objective lens and is attached to a Hitachi HV-F22 color camera and a Zeiss AxioCam MRm monochrome camera with a calibration scale. After scanning, images were viewed and captured analyzed using the Panoramic viewer software (3DHISTECH, Budapest, Hungary). CD31-stained endothelial cells served as a marker for blood vessel counting and CD68–macrophage and monocyte marker. Briefly: Antigen retrieval of the samples were performed via citrate-buffered solution in a microwave oven at two cycles of 5 min each, followed by blocking nonspecific binding sites with a block bluster (Background bluster, Innovex, Bioscience). After 2 $\times$ 5 min washes with PBS, the sections were incubated overnight in a humidified chamber with a primary antibody against CD31 (SP38, Novus Biologicals, USA), diluted 1:700 and CD68 (Biocare medical, CA, USA) diluted 1:4000. After extensive washing, samples were incubated with ABC–HRP antirabbit reagent (ZytoChem Plus HRP Polymer antirabbit, Zytomed system, Berlin, Germany) for 30 min, then washed with PBS three times, 2 min each. A working solution of DAB (DAB substrate kit, Zytomed, DAB057, Berlin, Germany) was prepared and applied for 7 min and gently washed with distilled water. Finally, sample dehydration and mounting were performed. Slides were visualized with an Olympus CX31 microscope (Olympus CX31, Olympus Optical, Philippines) equipped with an Olympus DP12 camera.

Statistical analysis

The StatPlus®5.7.8 statistical package (AnalystSoft, Vancouver, BC, Canada) was used. Descriptive statistics, including means, medians, ranges and standard deviation (SD). Comparison between test scaffolds (incorporated with rhVEGF$_{165}$) and

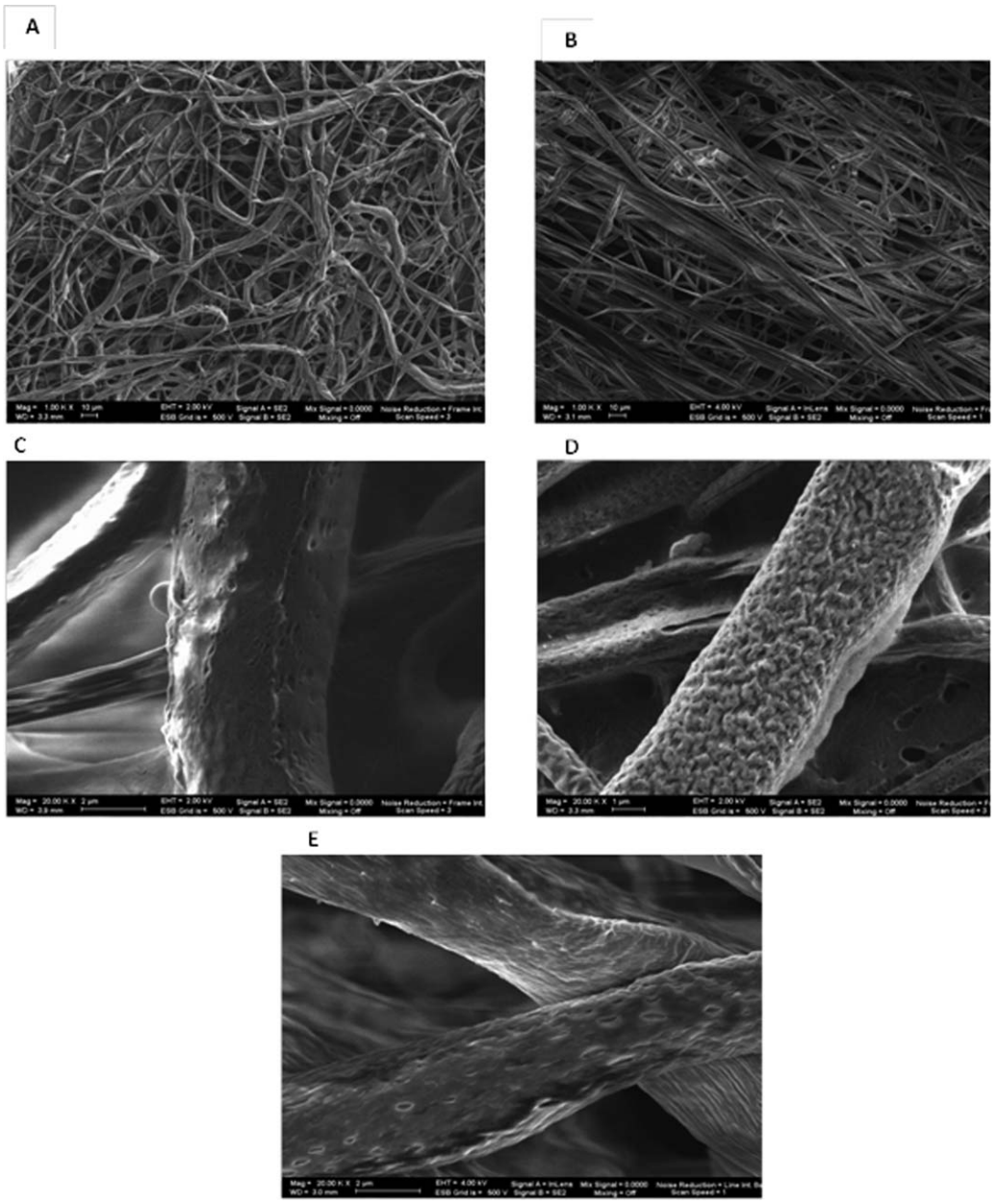

FIGURE 2. Electrospun core–shell scaffold pore size as a function of PEG concentration. A–B: SEM micrographs (×1000 magnification) of scaffolds with different PEG concentrations. A: 1% PEG, B: 3% PEG. C–E: SEM micrographs (×20,000 magnification) of scaffolds with different PEG concentrations: 0.25, 1, and 3% PEG, respectively.

control scaffolds (without VEGF) was performed using a Student's *t* test for unpaired observation (two-tailed). A threshold *pf* $p < 0.05$ was set to determine true significance.

RESULTS

Fabrication and characterization of core–shell fiber scaffolds incorporated with rhVEGF165

The electrospun core–shell nanofibers, containing varying concentrations of PEG (S1–0.25%, S2–1%, S3–3% PEG), exhibited a 6–8 μm diameter, although thinner and thicker fibers were also observed (Fig. 2). The 3% PEG polymeric scaffolds presented a higher mean pore size, higher pore density and smaller interfiber spaces, when compared with the 0.25 and 1% PEG polymeric scaffolds (Table I). Mean pore size was 204.976 ± 59.649 nm for the 0.25% PEG polymeric scaffold and 503.49 ± 64.57 nm for the 3% PEG polymeric scaffold (Table I; $p < 0.05$). Pore density ranged between $2.3/\mu m^2$ in 0.25% PEG polymeric scaffolds to $13.9/\mu m^2$ in 3% PEG polymeric scaffolds ($p < 0.05$). Interfiber spaces were threefold higher in 0.25 and 1% PEG polymeric scaffolds as compared to the 3% PEG polymeric scaffolds (Table I, $p < 0.05$).

Release kinetics of VEGF from the scaffold

Analysis of the temporal release of $rhVEGF_{165}$ from the fabricated nanofibers demonstrated that the 3% PEG polymeric

TABLE I. Pore Size and Pore Density of Scaffolds with Different PEG Concentrations

Scaffold #	Shell Solution Composition	Core Solution Composition	Pore Density ($1/\mu m^2$) Mean	Pore Diameter (nm) Mean ± SD	Interfibers Space (μm) Mean ± SD
S1	8% PCL 80 kþ 0.25% PEG 6 k in CHCl3/DMF 8:2	4% PEO 600k in water	2.3†	205 ± 60	20.714 ± 6.33
S2	8% PCL 80 kþ 1% PEG 6 k in CHCl3/DMF 8:2	4% PEO 600k in water	7.83*	225.5 ± 75	21.804 ± 10.67
S3	8% PCL 80 kþ 3% PEG 6 k in CHCl3/DMF 8:2	4% PEO 600k in water	13.8	503.5 ± 64.5††	8.066 ± 2.844††

DMF, dimethyl formamide; PEO, poly(ethylene oxide); PCL, polycaprolactone; PEG, poly(ethylene glycol).
†$p < 0.05$, S1 vs. other.
*$p < 0.05$, S2 vs. other.
††$p < 0.05$, S3 vs. other groups.

scaffolds released 23% of the loaded rhVEGF$_{165}$ content within 4 hours, with a burst release of approximately 65% of the total released rhVEGF$_{165}$ occurring during the first hour. The 0.25% PEG and 1% PEG polymeric scaffolds released approximately 38% of the loaded VEGF within 18 h, with the 1% PEG exhibiting a steeper release gradient in the first hour as compared to the 0.25% PEG polymeric scaffold (Fig. 3).

Due to the release kinetics demonstrated by the 1% PEG polymeric scaffold, with an initial burst release of hVEGF$_{165}$, followed by continuous release of the growth factor, this scaffold was used in all further experiments.

Cells adhesion to the scaffold

Twenty four hours after MSCs seeding on to the fabricated scaffold, cells had dispersed, adhered and spread on the scaffold. 3D modeling of the images demonstrated intimate contacts between cells (labelled with green CFSE) and the nanofiber scaffold (stained red Dil dye) (Fig. 4).

rhVEGF$_{165}$ released from the electrospun scaffolds enhance EC migration

A trans-well migration assay was performed to analyze whether the constructed scaffold preserved the biofunctionality of the incorporated hVEGF$_{165}$, and to determine if a slow-release pattern from the polymeric scaffold is superior to burst application of identical concentrations of the growth factor. EBM enriched with rhVEGF$_{165}$ (5 ng/mL) induced cell migration from the upper chamber toward the lower one through the porous membrane, while VEGF-free EBM had no effect on endothelial cell migration. The rhVEGF$_{165}$-incorporated scaffold (1% PEG) also successfully induced cell passage through the membrane. The continuous release of rhVEGF$_{165}$ from the scaffold increased the number of cells that passed through the membrane by 87-fold, compared to the EBM alone. In addition, it provided for a 5.89-fold increase in cell migration as compared to EBM enriched with rhVEGF165 (Fig. 5; Table II; $p = 0.00228$).

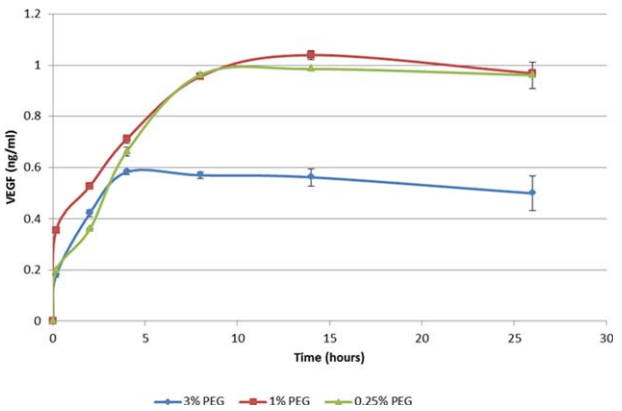

FIGURE 3. Graph demonstrating the release kinetics of VEGF from the scaffold. 1% PEG exhibited a steeper release gradient in the first hour as compared to the 0.25% and 3% PEG polymeric scaffold with approximately 38% of the loaded VEGF released within 18 h.

Implanted rhVEGF$_{165}$-incorporated scaffolds induce angiogenesis

A subcutaneous mouse model was used to assess the *in vivo* angiogenic potential of the fabricated and rhVEGF$_{165}$-incorporated scaffold. All mice survived the surgical procedure, and no complications were observed. 3 days after implantation, macroscopic evaluation of the extracted scaffolds showed no visible blood vessels (Fig. 6). However, 2 weeks after implantation, blood vessels covered the entire surface of the rhVEGF165-incorporated scaffolds, whereas the control scaffolds showed no signs of vasculature (Fig. 6).

Blood vessel density was examined using confocal microscopy and immunohistochemistry.

Confocal imaging. Scaffolds extracted 3 days post-transplantation showed no signs of functional vessels in either scaffold type (with or without rhVEGF165). However, both scaffolds successfully recruited cells, although the number of cells that had adhered to the rhVEGF$_{165}$ scaffold was greater than the number that adhered to the VEGF-free scaffold ($p < 0.05$; Fig. 6).

Functional blood vessels were observed in rhVEGF$_{165}$-incorporated scaffolds 2 weeks after subcutaneous implantation, while the control group did not contain functional vessels (Table III).

Immunohistochemistry. Blood vessel density and diameters were determined from the CD31-stained slides. Histological

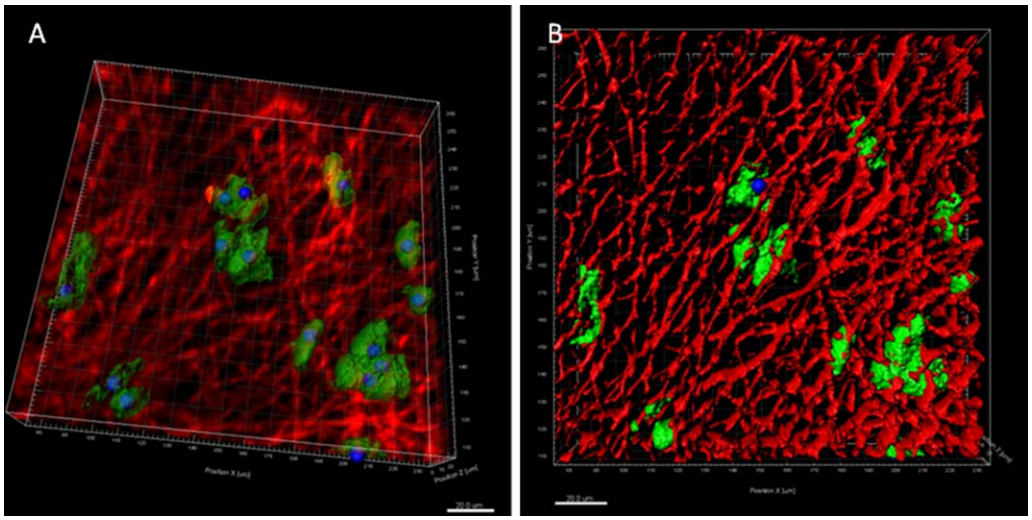

FIGURE 4. Laser confocal microscopy of electrospun nanofibers (A, B). Images were processed with Imaris software. Cells seen dispersed throughout and adhered to the scaffold. 3D modeling of the images demonstrate intimate contacts between the cells (labeled with green and blue) and the nanofiber scaffold (stained red).

and immunostaining of the specimens provided supporting evidence for the macroscopic observations and confocal imaging of functional vessels after 3 days, however slight differences were found after 14 days. Histological sections of scaffolds extracted 3 days after implantation showed small capillaries in the rhVEGF$_{165}$-incorporated scaffolds only, while in the control group, no blood vessels were detected. 2 weeks after implantation, the rhVEGF$_{165}$-incorporated scaffolds contained

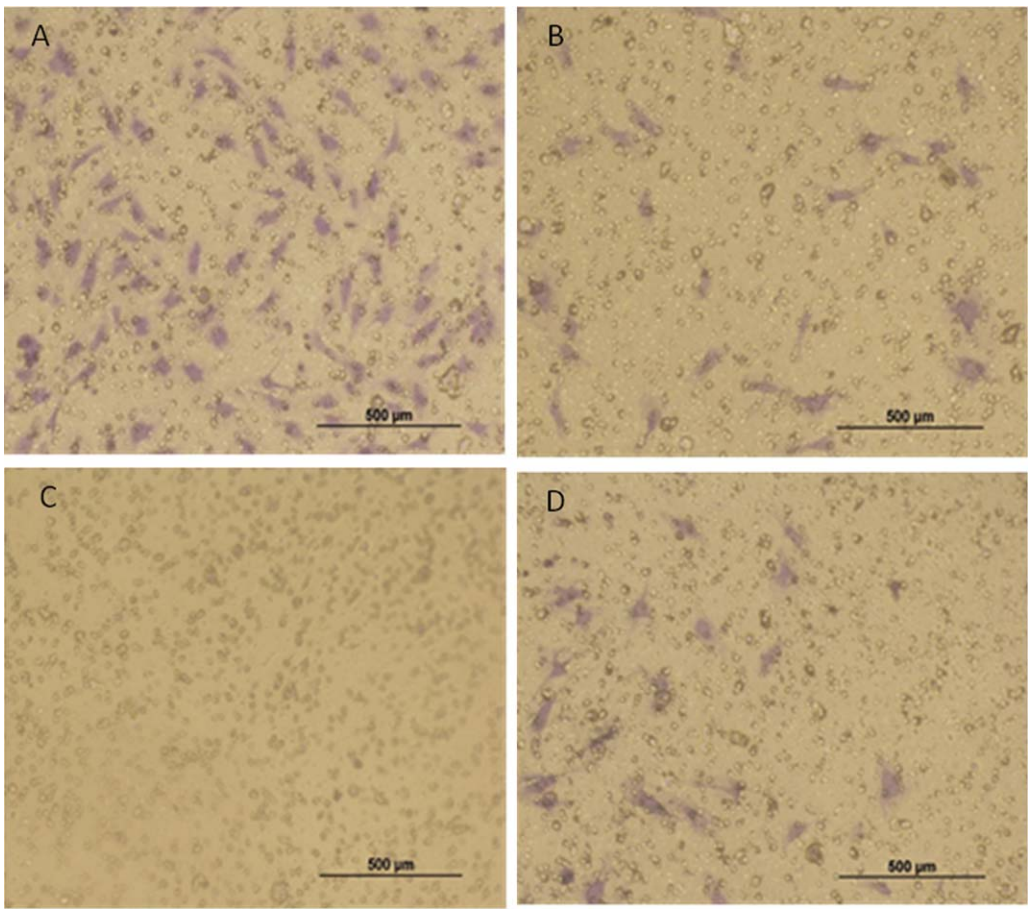

FIGURE 5. Transwell migration of ECs: Endothelial cells were seeded on top of a porous membrane, and migrated toward the lower chamber which contained: (A) scaffold incorporated with 15 ng/cm^2 rhVEGF165, soaked in EBM without supplements, B: a VEGF-free scaffold soaked in EBM without supplements. C: EBM without supplements, and D: EBM with 5 ng/mL rhVEGF$_{165}$.

TABLE II. Quantification of the EC Migration from rhVEGF-Impregnated Scaffolds Through the Trans-Well Membrane

Lower Chamber Content	Scaffold Releasing rhVEGF	Scaffold Soaked in EBM (VEGF–)	EBM + rhVEGF (5 ng/mL)	EBM Without VEGF
Ratio (violet color area/area) Mean ± SD	0.04382 ± 0.022012*	0.005062 ± 0.003288	0.007724 ± 0.00526†	0.001639 ± 0.002398

*p values < 0.05 versus all other groups †p values < 0.05 versus EBM without VEGF.

well developed blood vessels of large diameter (39 ± 3.1 μm), whereas in the VEGF-free scaffolds, blood vessels were scarce and narrow (14 ± 2.59 μm) (Fig. 7).

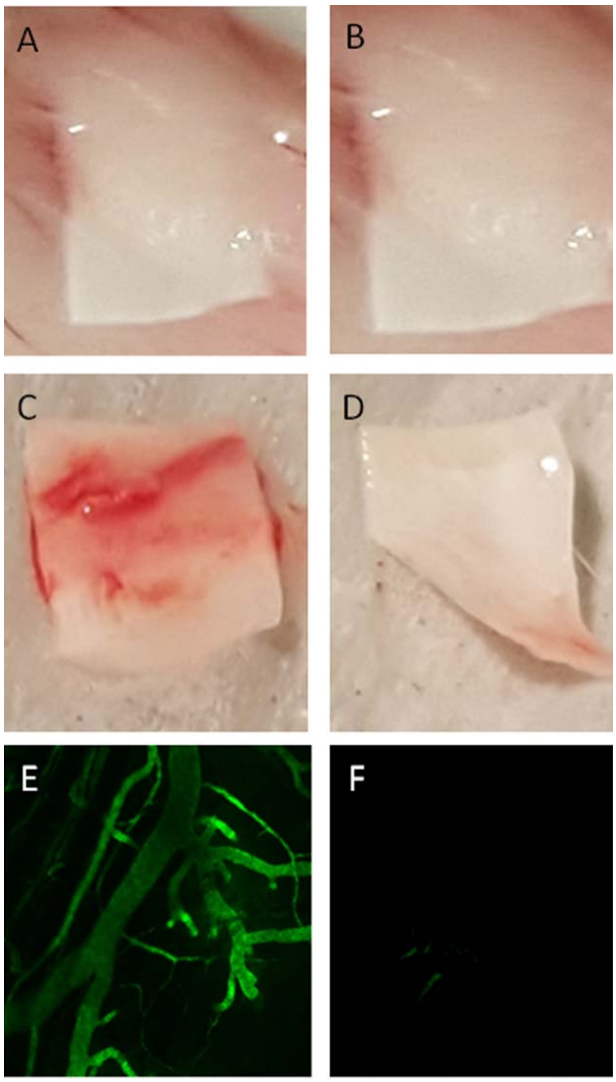

FIGURE 6. Macroscopic evaluation of electrospun scaffolds extracted 3 (A, B) and 14 (C–F) days after implantation. None of the scaffolds contained visible blood vessels 3 days after implantation (A: test group, B: control group). (C, D) Macroscopic evaluation at 14 days: Scaffolds incorporated with rhVEGF$_{165}$ displayed blood vessels running along the transplanted construct (C), whereas they were absent in the control group (D). (C: test group, D: control group). (E, F) Functional blood vessels were detected, using dextran in the rhVEGF$_{165}$ incorporated scaffold (E), but were absent in the control scaffolds (F) (LSM 510 Zeiss Laser scanning confocal system with 10× magnification).

rhVEGF$_{165}$-incorporated scaffolds did not elicit an inflammatory reaction

Specimens stained with CD68 at 3 and 14 days after implantation were negative, whereas, positive control (lymphoid tissue) stained positive. These results suggest that the rhVEGF$_{165}$-incorporated scaffolds did not elicit an inflammatory reaction (Fig. 8).

DISCUSSION

A novel nanofiber polymeric scaffold incorporated with rhVEGF$_{165}$ was designed to induce angiogenesis. The presented analyses demonstrated that rhVEGF$_{165}$ can be incorporated within the aqueous core solution of an electrospun fibrous core–shell scaffold. Moreover, the protein was successfully released from the fabricated scaffold via pores in the outer shell. An *in vitro* trans-well migration assay showed that the released rhVEGF$_{165}$ maintained its biological activity and successfully induced endothelial cell migration. In addition, when subcutaneously transplanted into mice, the scaffold induced angiogenesis.

Previous studies have successfully incorporated rhVEGF$_{165}$ into scaffolds fabricated from PLGA[8] and collagen–hydroxyapatite.[21] In both studies, VEGF enhanced neovascularization and bone regeneration following transplantation into bone defects. To the best of our knowledge, this is the first report of an electrospun core–shell fibrous scaffold incorporated with rhVEGF$_{165}$. The electro-spinning technology provides the ability to control the shape of the scaffold by changing the shape of the collector. In addition, the polymeric components used in our system are biocompatible and approved for clinical use.[22] PCL is degraded by hydrolysis of its ester linkages under physiological conditions and has therefore received a great deal of attention for its applicability as an implantable biomaterial. PCL has been approved by the Food and Drug Administration (FDA) for neurosurgery[23,24] and orthopedic devices.[25] In parallel, PEG is already in extensive clinical use, in applications such as a protein delivery devices.[26] Currently, PEG is the polymer most widely used as a degradeable carrier in protein therapeutics. It is inert, inexpensive, has low toxicity and has been approved by the FDA.[27] Incorporating PEG frequently reduces both immunogenicity and antigenicity of proteins, which arise from the shielding effect of the PEG chains on the antigenic determinants of the proteins.[28] Therefore, proteins that are protected by PEG does elicit antibody formation, the antibodies bear a weaker affinity to the protein compared with native proteins.[29] Indeed, in the current study no inflammatory reaction was detected. Although the PEG dissolved after transplantation, there may be remnants in the scaffold that provide the shielding

TABLE III. Functional Blood Vessels in Extracted Scaffolds 14 Days After Subcutaneous Transplantation

	Total Blood Vessels Diameter (μm)	Number Blood Vessels Branches	Total Blood Vessels Volume (μm^3)	Total Blood Vessels Length (μm)	Total Blood Vessels Area (μm^2)
rhVEGF165impregnate scaffold	32 ± 6	$4.47 \times 10^3 \pm 2.28 \times 10^3$	$4.699 \times 10^6 \pm 4.07 \times 10^5$	$4.49 \times 10^3 \pm 2.78 \times 10^3$	$4.96 \times 10^5 \pm 3.694 \times 10^4$
Scaffold free VEGF	0	0	0	0	0
p value	0.000001	0.000001	0.000001	0.000001	0.000001

effect. Alternatively, SCID mice have an impaired immune response.

An additional advantage of electrospun core–shell systems lies in the close structural resemblance between the fabricated 3D nanofibers and extracellular matrix. The elongated electrospun fibers resemble collagen fibers, and their diameter and interfiber spaces allow for easy adherence of cells, and provide a suitable porous structure and substrate for blood vessel growth.[30] However, the most central advantage of the described electrospun core–shell system lies on its ability to control the release of $rhVEGF_{165}$ by manipulating PEG concentrations to fit the desired release profile. A positive correlation between PEG concentrations in the scaffold and pore size in the outer shell of the fibers was observed, with 3% PEG providing for a mean pore size double that obtained in 1% PEG polymeric scaffolds. Moreover, the PEG concentration influenced the release kinetics of $rhVEGF_{165}$, as demonstrated by ELISA. Since $rhVEGF_{165}$ release from the scaffold depends on effective diffusion,[31,32] larger pore sizes facilitate $rhVEGF_{165}$ release. However, the 3% PEG polymeric scaffolds demonstrated lower total VEGF release as compared to the 1 and 0.25% PEG polymeric scaffolds. These results can be attributed to the adsorption of VEGF to contaminated PCL that might occur in systems with high PEG concentrations.

The release profile is another important factor that must be considered when designing a novel delivery system. Considering that the half-life of most growth factors in serum is very short, and for $rhVEGF_{165}$ is 33.7 ± 13.7 min,[2,13] in order to initiate and maintain biological responses, it is essential for bioactive scaffolds to preserve the desired protein

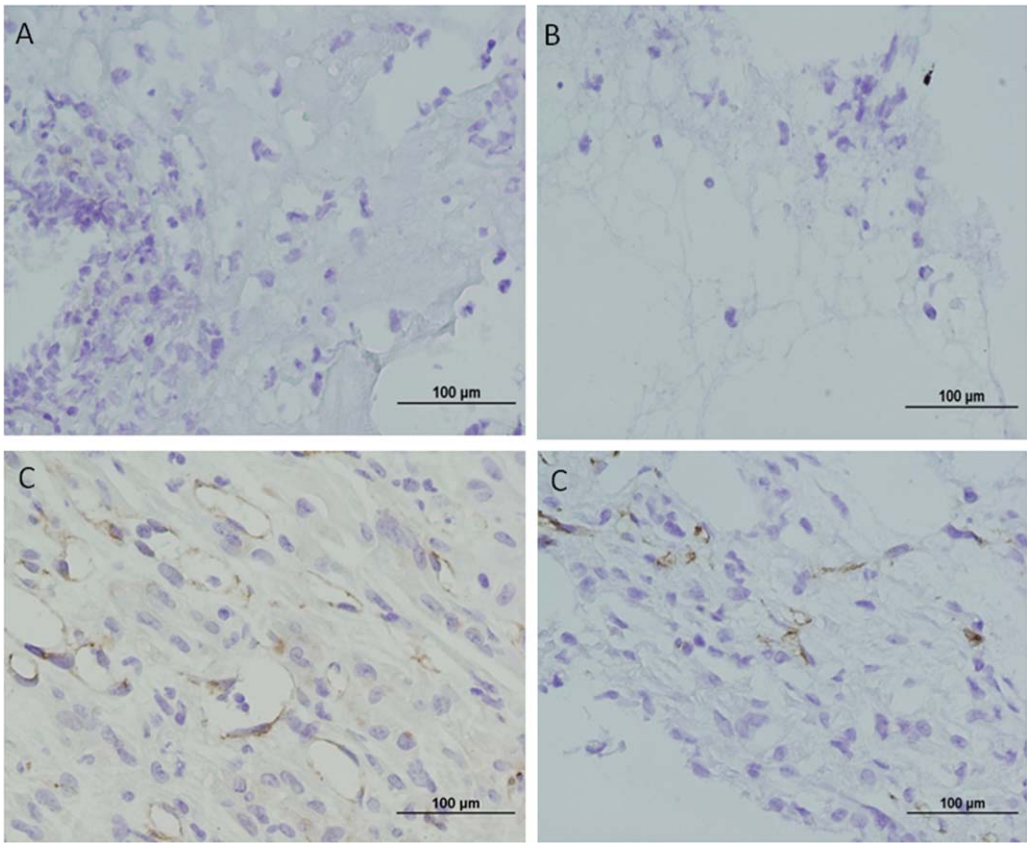

FIGURE 7. CD31 positive blood vessels in subcutaneous implanted scaffolds: At 3 days, no blood vessels were detected in $rhVEGF_{165}$-incorporated scaffolds (A) or in VEGF-free scaffolds (B). At 2 weeks, $rhVEGF_{165}$-incorporated scaffolds showed well developed blood vessels (C) whereas blood vessels were barely detected in the $rhVEGF_{165}$-free scaffold (D) (3D Histech Pannoramic MIDI scanner with 20× magnification).

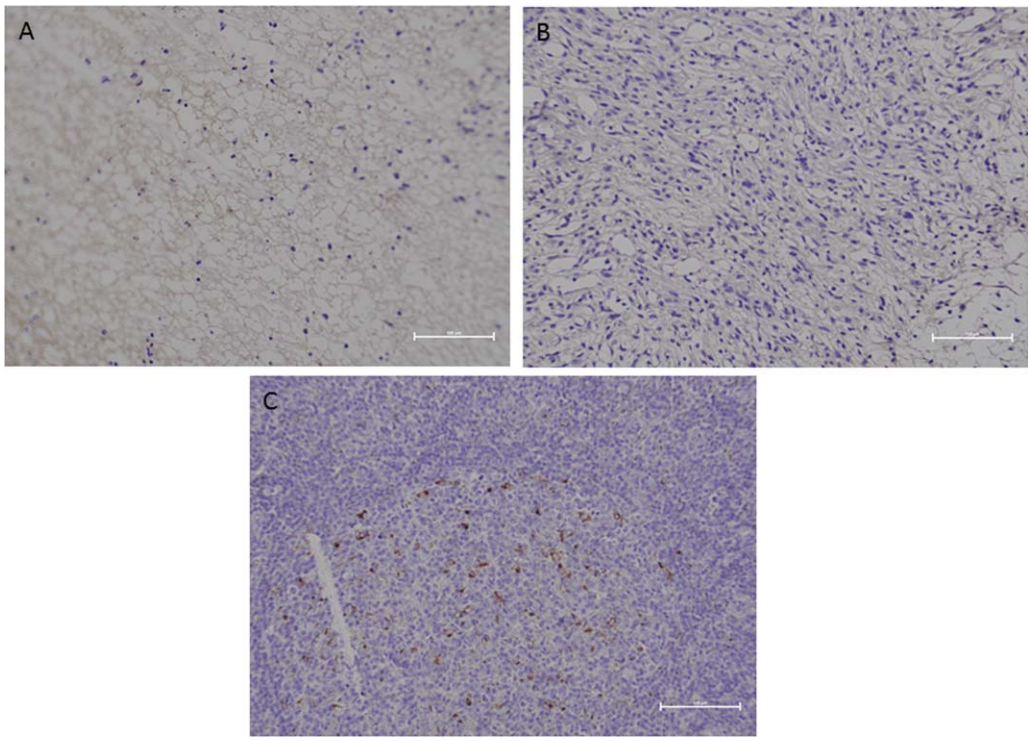

FIGURE 8. CD68 (macrophage and monocyte marker) was negative after 3 (A) and 14 (B) days after implantation but positive in the lymphoid tissue, and (C) positive control.

concentration for extended periods of time. For this purpose, an optimal growth factor-delivering scaffold should be able to initially release a high fraction of the loaded protein, which is typically termed a "burst release",[33] to rapidly achieve the effective therapeutic concentration. Subsequently, well-defined slow-release kinetics should follow, in order to maintain the effect.[34] Our ELISA results demonstrated that the fabricated, rhVEGF$_{165}$-incorporated scaffolds successfully fulfilled this requirement. Our experiments focused on 1% PEG polymeric scaffolds, as they released approximately 38% of the loaded rhVEGF$_{165}$ within 18 h, with a burst release during the first hour, a release profile most suitable for angiogenesis stimulation via rapid cell recruitment.[33,34]

Preservation of the stability and bioactivity of biomolecules incorporated within scaffolds is one of the major challenges in fabricating delivery systems. During scaffold fabrication and storage, the incorporated protein is subjected to chemical and physical stress. In our study, the use of PEO as the core material ensured the stability of rhVEGF$_{165}$, by minimizing hydrophobic interactions between the organic solvents (PEO) and rhVEGF$_{165}$ during the electrospinning process.[35,36] Additionally, the use of a coaxial electrospinning method kept electric charges predominantly on the outer surface of the fiber, leaving the rhVEGF$_{165}$ in the inner solutions uncharged and stable for a longer duration of time.[37] The *in vitro* trans-well migrations results demonstrated that the bioactivity of hVEGF$_{165}$ in the scaffold was preserved and that the migration of ECs toward the scaffold was influenced by the rhVEGF$_{165}$ release kinetics. The trans-well migration assay showed enhanced migration (5.89-fold higher) of ECs in response to gradual release of rhVEGF$_{165}$ from the 1% PEG polymeric scaffold, as compared to a single application of rhVEGF$_{165}$ in a similar concentration. An additional confirmation of preservation of rhVEGF$_{165}$ bioactivity in the scaffold was provided upon subcutaneous implantation of the scaffold into mice. Recruitment of cells to the scaffold was observed within 3 days and was higher in the rhVEGF$_{165}$-incorporated scaffolds compared to control scaffolds ($p < 0.05$). Moreover, 2 weeks after subcutaneous implantation, new functional blood vessels were observed in the rhVEGF165-incorporated scaffolds, while in the control group, blood vessels were scarce and of smaller diameters.

While this study presents promising results, there are still several limitations. The growth factor release kinetics of our delivery system is likely to be affected by many factors, including polymer swelling, biomolecular dissolution/diffusion, biomolecule distribution inside the matrix and biomolecule/polymer ratios.[34] Therefore, it is difficult to find a single mathematical equation that can predict the controlled release profile of an incorporated protein. Another limitation of our scaffold is the relatively low percentage of rhVEGF$_{165}$ that was released (38%). Additional methods will have to be adopted to maximize rhVEGF$_{165}$ release from the core solution.

In summary, the current study demonstrated the feasibility of construction of core–shell coaxially electrospun fibrous scaffolds that allow for slow release of rhVEGF$_{165}$ to promote angiogenesis. Further investigations will still be necessary to determine the optimal parameters for fabricating scaffolds to release VEGF, optimal VEGF concentrations

and release kinetics. This scaffold represents a promising tool for vascular tissue engineering, which may promote wound healing especially in cases of insufficient vasculature, such as in diabetic patients.

ACKNOWLEDGMENTS

We would like to thank Professor Eyal Zussman and Dr. Ron Avrahimi from the Faculty of Mechanical Engineering, Technion for their assistance with the scaffold fabrication, as well as, Dr. E. Suss Toby, M. Gurewitz, and L. Liba from the BCF Bioimaging Center (Faculty of Medicine, Technion) for their assistance with imaging and image analysis.

DISCLOSURE

The authors declare that they have no conflict of interest.

REFERENCES

1. Liu W, Thomopoulos S, Xia Y. Electrospun nanofibers for regenerative medicine. Adv Healthcare Mater 2012;1:10–25.
2. Jain RK, Au P, Tam J, Duda DG, Fukumura D. Engineering vascularized tissue. Nat Biotechnol 2005;23:821–823.
3. Wei G, Ma PX. Nanostructured biomaterials for regeneration. Adv Funct Mater 2008;18:3568–3582.
4. Berger J, Reist M, Mayer JM, Felt O, Peppas NA, Gurny R. Structure and interactions in covalently and ionically crosslinked chitosan hydrogels for biomedical applications. Eur J Pharm Biopharm 2004;57:19–3457.
5. Chan B, Leong K. Scaffolding in tissue engineering: general approaches and tissue-specific considerations. Eur Spine J 2008; 17:467–479.
6. Nobuto T, Imai H, Yamaoka A. Microvascularization of the free gingival autograft. J Periodontol 1988;59:639–646.
7. Koffler J, Kaufman-Francis K, Shandalov Y, Egozi D, Pavlov DA, Landesberg A, Levenberg S. Improved vascular organization enhances functional integration of engineered skeletal muscle grafts. Proc Natl Acad Sci 2011;108:14789–14794.
8. Kaigler D, Wang Z, Horger K, Mooney DJ, Krebsbach PH. VEGF scaffolds enhance angiogenesis and bone regeneration in irradiated osseous defects. J Bone Miner Res 2006;21:735–744.
9. Srouji S, Ben-David D, Lotan R, Livne E, Avrahami R, Zussman E. Slow-release human recombinant bone morphogenetic protein-2 embedded within electrospun scaffolds for regeneration of bone defect: *in vitro* and *in vivo* evaluation. Tissue Eng A 2010;17:269–277.
10. Liao S, Li B, Ma Z, Wei H, Chan C, Ramakrishna S. Biomimetic electrospun nanofibers for tissue regeneration. Biomed Mater 2006;1:R45.
11. Jiang B, DeFusco E, Li B. Polypeptide multilayer film co-delivers oppositely-charged drug molecules in sustained manners. Biomacromolecules 2010;11:3630–3637.
12. Hu J, Ma PX. Nano-fibrous tissue engineering scaffolds capable of growth factor delivery. Pharm Res 2011;28:1273–1281.
13. Eppler SM, Combs DL, Henry TD, Lopez JJ, Ellis SG, Yi JH, Annex BH, McCluskey ER, Zioncheck T. A target-mediated model to describe the pharmacokinetics and hemodynamic effects of recombinant human vascular endothelial growth factor in humans. Clin Pharmacol Ther 2002;72:20–32.
14. Sun Z, Zussman E, Yarin AL, Wendorff JH, Greiner A. Compound core–shell polymer nanofibers by co-electrospinning. Adv Mater 2003;15:1929–1932.
15. Dror Y, J, Kuhn Avrahami E. Zussman Encapsulation of enzymes in biodegradable tubular structures. Macromolecules 2008;41: 4187.
16. Tiwari SK, Tzezana R, Zussman E, Yizhong H, Venkatraman SS. Optimizing drug partitioning in electrospun core–shell fibres. Int J Pharm 2010;392:209–217.
17. Vasita R, Katti DS. Nanofibers and their applications in tissue engineering. Int J Nanomed 2006;1:15.
18. Ozawa CR, Banfi A, Glazer NL, Thurston G, Springer ML, Kraft PE, McDonald DM, Blau HM. Microenvironmental VEGF concentration, not total dose, determines a threshold between normal and aberrant angiogenesis. J Clin Investig 2004;113:516–527.
19. Dror Y, Salalha W, Avrahami R, Zussman E, Yarin AL, Dersch R, ... Wendorff JH. One-Step production of polymeric microtubes by co-electrospinning. Small 2007;3:1064–1073.
20. Costa-Pinto AR, Correlo VM, Sol PC, Bhattacharya M, Srouji S, Livne E, Reis RL, Neves NM. Chitosan-poly (butylene succinate) scaffolds and human bone marrow stromal cells induce bone repair in a mouse calvaria model. J Tissue Eng Regener Med 2012;6:21–28.
21. Sachlos E, Gotora D, Czernuszka JT. Collagen scaffolds reinforced with biomimetic composite nano-sized carbonate-substituted hydroxyapatite crystals and shaped by rapid prototyping to contain internal microchannels. Tissue Eng 2006;12:2479–2487.
22. Liu Y, Lim J, Teoh S-H. Review: development of clinically relevant scaffolds for vascularised bone tissue engineering. Biotechnol Adv 2013;31:688–705.
23. Schantz JT, Lim TC, Ning C, Teoh SH, Tan KC, Wang SC, Hutmacher DW. Cranioplasty after trephination using a novel biodegradable burr hole cover: technical case report. Oper Neurosurg 2006;58:ONS–E176.
24. Low SW, Ng YJ, Yeo TT, Chou N. Use of Osteoplug^{TM} polycaprolactone implants as novel burr–hole covers. Singapore Med J 2009;50:777–780.
25. Middleton JC, Tipton AJ. Synthetic biodegradable polymers as orthopedic devices. Biomaterials 2000;21:2335–2346.
26. Veronese FM, Pasut G. PEGylation, successful approach to drug delivery. Drug Discov Today 2005;10:1451–1458.
27. Molineux G. Pegylation: engineering improved pharmaceuticals for enhanced therapy. Cancer Treat Rev 2002;28:13–16.
28. Abuchowski A, Van Es T, Palczuk NC, Davis FF. Alteration of immunological properties of bovine serum albumin by covalent attachment of polyethylene glycol. J Biol Chem 1997;252:3578–3581.
29. Wieder KJ, Palczuk NC, van Es T, Davis FF. Some properties of polyethylene glycol: phenylalanine ammonia-lyase adducts. J Biol Chem 1979;254:12579–12587.
30. Li WJ, Laurencin CT, Caterson EJ, Tuan RS, Ko FK. Electrospun nanofibrous structure: a novel scaffold for tissue engineering. J Biomed Mater Res 2002;60:613–621.
31. Gandhi M, Srikar R, Yarin AL, Megaridis CM, Gemeinhart RA. Mechanistic examination of protein release from polymer nanofibers. Mol Pharm 2002;6:641–647.
32. Srikar R, Yarin AL, Megaridis CM, Bazilevsky AV, Kelley E. Desorption-limited mechanism of release from polymer nanofibers. Langmuir 2008;24:965–974.
33. Huang X, Brazel CS. On the importance and mechanisms of burst release in matrix-controlled drug delivery systems. J Control Release 2001;73:121–136.
34. Grassi M, Grassi G. Mathematical modelling and controlled drug delivery: matrix systems. Curr Drug Deliv 2005;2:97–116.
35. Wang Y, Annunziata O. Comparison between protein–polyethylene glycol (PEG) interactions and the effect of PEG on protein–protein interactions using the liquid–liquid phase transition. J Phys Chem B 2007;111:1222–1230.
36. Michel R, Pasche S, Textor M, Castner DG. Influence of PEG architecture on protein adsorption and conformation. Langmuir 2005; 21:12327–12332.
37. Pham QP, Sharma U, Mikos AG. Electrospinning of polymeric nanofibers for tissue engineering applications: a review. Tissue Eng 2006;12:1197–1211.